

# CHEM MED CHEM

CHEMISTRY ENABLING DRUG DISCOVERY

## Accepted Article

**Title:** Deciphering specificity determinants for FR900359-derived Gαq inhibitors based on computational and structure-activity studies

**Authors:** Diana Imhof, Raphael Reher, Toni Kühn, Suvi Annala, Tobias Benkel, Desiree Kaufmann, Britta Nubbemeyer, Justin P. Odhiambo, Pascal Heimer, Charlotte A. Bäuml, Stefan Kehraus, Max Crüseemann, Evi Kostenis, Daniel Tietze, and Gabriele M. König

This manuscript has been accepted after peer review and appears as an Accepted Article online prior to editing, proofing, and formal publication of the final Version of Record (VoR). This work is currently citable by using the Digital Object Identifier (DOI) given below. The VoR will be published online in Early View as soon as possible and may be different to this Accepted Article as a result of editing. Readers should obtain the VoR from the journal website shown below when it is published to ensure accuracy of information. The authors are responsible for the content of this Accepted Article.

**To be cited as:** *ChemMedChem* 10.1002/cmdc.201800304

**Link to VoR:** <http://dx.doi.org/10.1002/cmdc.201800304>

WILEY-VCH

[www.chemmedchem.org](http://www.chemmedchem.org)

A Journal of



# Deciphering specificity determinants for FR900359-derived Gαq inhibitors based on computational and structure-activity studies

Raphael Reher,<sup>#[a]</sup> Toni Kühl,<sup>#[b]</sup> Suvi Annala,<sup>[c]</sup> Tobias Benkel,<sup>[c]</sup> Desireé Kaufmann,<sup>[d]</sup> Britta Nubbemeyer,<sup>[b]</sup> Justin Patrick Odhiambo,<sup>[b]</sup> Pascal Heimer,<sup>[b]</sup> Charlotte Anneke Bäuml,<sup>[b]</sup> Stefan Kehraus,<sup>[a]</sup> Max Crüsemann,<sup>[a]</sup> Evi Kostenis,<sup>[c]</sup> Daniel Tietze,<sup>\*[d]</sup> Gabriele M. König,<sup>\*[a]</sup> and Diana Imhof<sup>\*[b]</sup>

- [a] R. Reher, Dr. S. Kehraus, Dr. M. Crüsemann, Prof. Dr. G. M. König  
Institute of Pharmaceutical Biology, University of Bonn, Nussallee 6, 53115 Bonn, Germany Department  
University of Bonn  
Nussallee 6, 53115 Bonn, Germany  
E-mail: g.koenig@uni-bonn.de  
ORCID: 0000-0003-0003-4916 (Prof. Dr. G. M. König), 0000-0001-6660-2715 (Dr. M. Crüsemann)
- [b] Dr. T. Kühl, B. Nubbemeyer, J. P. Odhiambo, Dr. P. Heimer, C. A. Bäuml, Prof. Dr. D. Imhof  
Pharmaceutical Biochemistry and Bioanalytics  
Pharmaceutical Institute  
University of Bonn  
An der Immenburg 4, 53121 Bonn, Germany  
E-mail: dimhof@uni-bonn.de  
ORCID: 0000-0003-4163-7334 (Prof. Dr. D. Imhof)
- [c] S. Annala, T. Benkel, Prof. Dr. E. Kostenis  
Molecular, Cellular and Pharmacobiology Section  
Institute of Pharmaceutical Biology  
University of Bonn  
Nussallee 6, 53115 Bonn, Germany  
ORCID: 0000-0001-8284-5514 (Prof. Dr. E. Kostenis), 0000-0002-2764-299X (S. Annala)
- [d] D. Kaufmann, Dr. D. Tietze  
Eduard Zintl Institute for Inorganic and Physical Chemistry  
Technische Universität Darmstadt  
Alarich-Weiss-Str. 4, 64287 Darmstadt, Germany  
E-mail: tietze@chemie.tu-darmstadt.de  
ORCID: 0000-0002-9251-1902 (Dr. D. Tietze)

Supporting information for this article is given via a link at the end of the document.

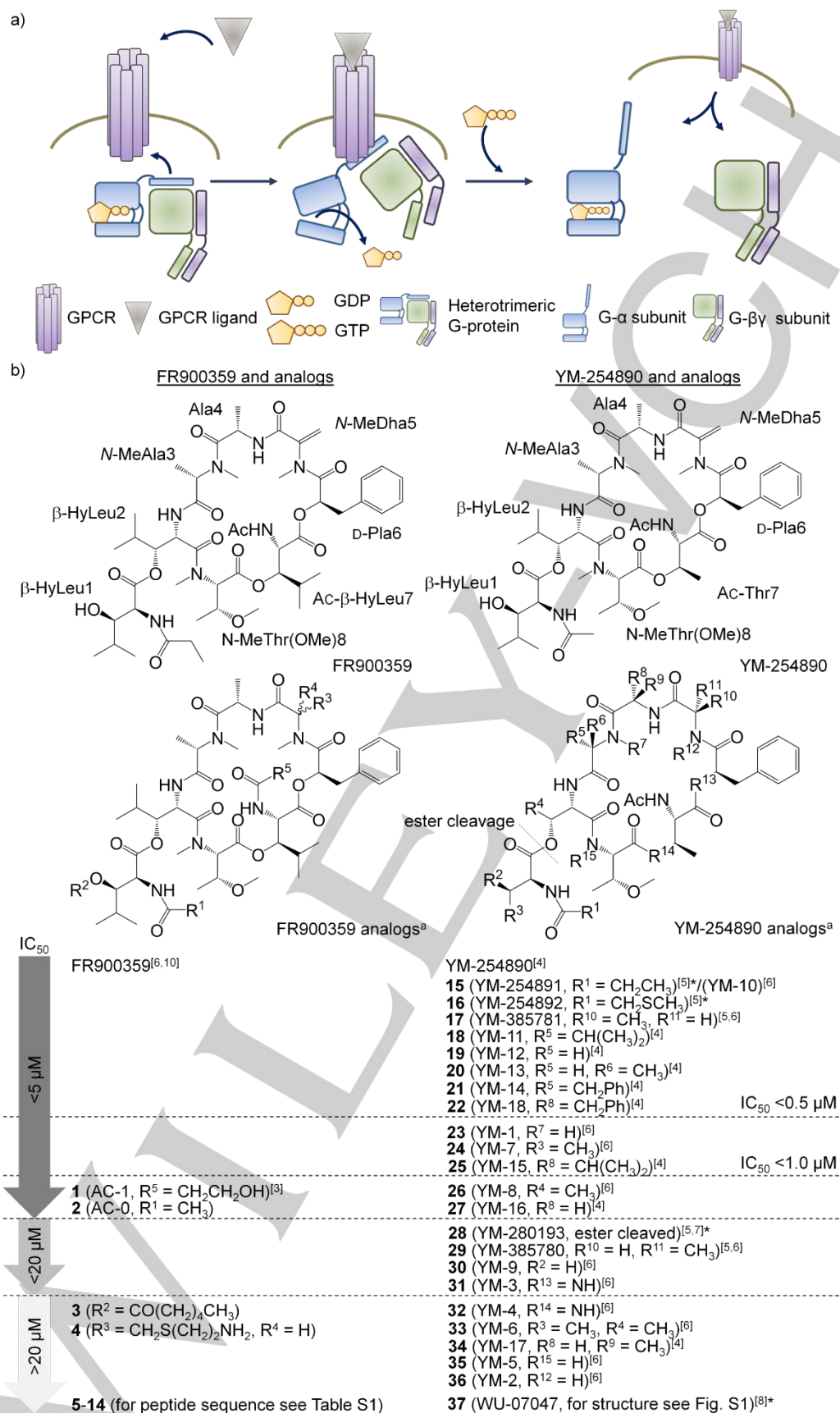
**Abstract:** Direct targeting of intracellular Gα subunits of G protein-coupled receptors by chemical tools represents a challenging task in current pharmacological studies and developing novel therapeutic approaches. Here we analyzed novel FR900359-based analogs from natural sources, synthetic cyclic peptides as well as all so-far known Gαq inhibitors in a comprehensive study to devise a strategy for the elucidation of characteristics that determine interaction with and inhibition of Gαq in the specific FR/YM binding pocket. Using 2D NMR spectroscopy and molecular docking we have identified unique features in the macrocyclic structures responsible for binding to the target protein correlating with inhibitory activity. While all novel compounds were devoid of effects on Gi and Gs proteins, no inhibitor surpassed biological activity of FR. This raises the question of whether depsipeptides such as FR already represent valuable chemical tools for specific inhibition of Gαq and, at the same time, are suitable natural lead structures for the development of novel compounds to target Gα subunits other than Gαq.

## Introduction

Heterotrimeric (Gαβγ) G proteins represent one of the most important components of intracellular signaling cascades required for signal transduction by G protein-coupled receptors (GPCRs).<sup>[1,2]</sup> GPCR stimulation and subsequent G protein activation promotes the exchange of GDP/GTP at the Gα

subunit (Scheme 1a). After signal propagation, the GTP of the active state (GTP-bound Gα) is hydrolyzed to GDP resulting in the GDP-bound inactive form (GDP-bound Gα).<sup>[3-10]</sup> Apart from these forms the so-called “empty-pocket” conformation (nucleotide-free conformation, Scheme 1a) has been suggested to be stabilized upon interaction of BIM-46187 with Gαq.<sup>[11]</sup> Modulators of G protein function such as BIM-46187 are very important pharmacological tools to approach G protein-mediated signaling. In this context, the cyclic depsipeptides YM-254890 (YM) and FR900359 (FR), derived from bacterial strain *Chromobacterium* sp. QS3666<sup>[12-14]</sup> and the bacterial leaf nodule symbiont *Candidatus Burkholderia crenata* of the evergreen plant *Ardisia crenata* Sims,<sup>[3,10,15,16]</sup> respectively, take on an exceptional position among G protein inhibitors. Both compounds are able to selectively interfere with the function of Gαq/11 of GPCRs<sup>[12,15,17]</sup> representing the only potent and cell permeable inhibitors available so far. In brief, YM and FR act as guanine nucleotide dissociation inhibitors (GDI) by preventing GDP release due to conformational changes of the helical and Ras domains of Gαq.<sup>[14,15]</sup>

Due to the crucial role played by G proteins concerning GPCR signaling and a variety of diseases,<sup>[9,18]</sup> YM, FR, and respective analogs have a high pharmaceutical potential. The natural compounds were obtained by isolation from the biological material,<sup>[10,12]</sup> however, also a strategy for the total chemical synthesis of YM was reported by Xiong et al. in 2016.<sup>[6]</sup> Although a small number of analogs such as WU-07047,<sup>[8]</sup> YM-280193,<sup>[7]</sup>



**Scheme 1.** a) Activation states of G proteins presenting closed, empty pocket and open confirmation occurring during GDP to GTP nucleotide exchange. b) Structures and activities of FR900359 (left), YM-254890 (right), and corresponding analogs from these and previous studies.<sup>[3–8,10]</sup> Compounds are listed based on their reported IC<sub>50</sub> values determined by inhibition of carbachol-induced IP<sub>1</sub> production where available (Compounds measured with other assays are marked with an asterisk). <sup>a</sup>Chemical modifications relative to FR and YM are given in brackets (R<sup>1</sup>–R<sup>15</sup>) for the corresponding compound.

and others<sup>[4,6]</sup> (Scheme 1b) were reported earlier, a detailed analysis of the structure-activity relationships (SAR) of these compounds with respect to Gq (Gq) and other G proteins is still missing. The major reason for this is the lack of NMR structural analysis of suitable compounds together with a detailed in-silico analysis which enables the visualization of the recognition mode of ligand-Gq protein interaction. Here we report an in-depth analysis of the interaction of differentially active and inactive analogs of YM and FR, respectively, derived from either isolation from biological material or chemical synthesis, with the Gq protein. Moreover, all analogs described so far were included in the present study in order to derive key molecular properties for binding to and inhibition of Gq.

As the total synthesis of YM-254890 and several derivatives was published recently,<sup>[4,6]</sup> and further analogs are presented in this study, the thorough analysis of structural determinants for Gq protein binding and inhibition is now in place. Therefore, we first grouped 14 new FR- and YM-derived compounds as well as all 23 already published analogs according to their potency, to identify tolerated, partially tolerated, non-tolerated minor, and non-tolerated major modifications in the original sequence(s) (Scheme 1b). Biological activities for YM, FR and compounds 15–37 (Scheme 1b) vary somewhat due to different methods used for determining biological activity in various laboratories. We thus only refer to the herein determined values.<sup>[19]</sup>

## Results and Discussion

### Novel natural, semisynthetic, and synthetic FR900359 analogs.

FR contains an acetylated  $\beta$ -hydroxy-leucine residue instead of an acetylated threonine in the cyclic part, and a propionate unit in place of an acetate acyl residue located at the side chain as compared to YM (Scheme 1b). Such depsipeptides are produced by non-ribosomal peptide synthetases (NRPS), biosynthetic machineries which are known to produce - apart from their major product (here FR, YM) - also minor compounds due to some promiscuity of the biosynthetic enzymes.<sup>[3,20]</sup> Indeed, Taniguchi et al. were able to isolate additional YM derivatives (15, 16, 28, Scheme 1b) from the culture broth of *Chromobacterium* sp. QS3666.(5) MS/MS measurements of our *A. crenata* extracts showed the presence of FR analogs, which were successfully isolated from the plant material (compounds 1 and 2, Tables S1, S2, Figures S1–S3). 1 (AC-1) and 2 (AC-0) differ from native FR with respect to their acylation pattern (Figure S1).<sup>[3]</sup> Since compound 2 has not been described yet, a detailed NMR and MS/MS analysis has been performed herein (Table S2, Figure S3). Furthermore, an alternative approach to obtain related compounds was based on the semisynthesis of FR analogs yielding 3 and 4 (Figures S4, S5, Tables S1, S2). Analog 3 and 4 were obtained either by esterification of the  $\beta$ -HylLeu1 hydroxyl group with hexanoic anhydride (3) or by Michael addition applying 2-aminoethanethiol hydrochloride to form the corresponding thioether at the double bond of *N*-MeDha (4). MS/MS analysis revealed successful generation of 3 and 4 (Figures S3–S5). The naturally occurring compounds 1 and 2 were obtained in acceptable, even though low yields (0.00005–0.0005%) from dried *A. crenata* leaves and used together with semisynthetic 3 and 4 (yields 13.5% and 30%, respectively) for SAR studies.

Complexity and low yields of depsipeptide syntheses encouraged several groups to provide simplified and more easily accessible analogs of YM or FR,<sup>[4,6–8]</sup> which can be exemplified with WU-07047 (37),<sup>[6]</sup> YM-280193 (28),<sup>[7]</sup> and the recently reported 18 YM-analogs (15, 18–27, 30–36, Scheme 1b).<sup>[4,6]</sup> In attempts to design new analogs, we intended to keep basic features of YM/FR, while at the same time introducing more complex changes in our peptide series (5–14, Scheme 1b, Tables S1, S2). These peptides were synthesized according to standard Fmoc-protocol on a solid support and cyclized by head-to-tail cyclization in solution using PyBOP as coupling reagent.<sup>[21]</sup>

### Inhibitory activity of FR900359-derived analogs and peptides.

The depsipeptides 1–4 and peptides 5–14 were tested for their inhibitory activity, not representing quantitative binding affinity data, on second messenger-generating Gq, Gs, and Gi signaling pathways, respectively (Figure 1, Figure S6). The analysis of Gq-mediated signaling was accomplished by measuring the formation of second messenger D-myo-inositol 1-phosphate (IP1) upon stimulation of Gq-linked muscarinic M1 receptor with carbachol in stable CHO-M1 transfectants. Analog 1 and 2 were in the same activity range (1.0–1.8  $\mu$ M) as the lead compounds FR and YM (Scheme 1b, Table S1, Figure 1). The values of FR and YM determined in our study represent a direct head-to-head comparison relative to our analogs. Deviation from reported data<sup>[4,6]</sup> occur due to different assay protocols and assay sensitivity. Surprisingly, depsipeptide 3 only revealed an IC<sub>50</sub> value of ~90  $\mu$ M, while compound 4 and peptides 5–14 were inactive at Gq. In addition, no Gs or Gi activity was observed as determined in second messenger cAMP accumulation assays for all compounds 1–14 (data not shown).

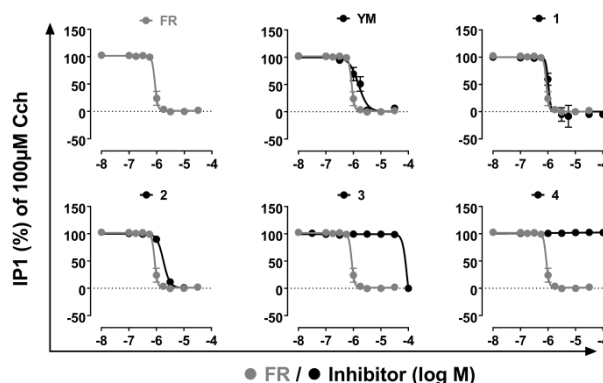


**Figure 1.** Carbachol-induced IP<sub>1</sub> accumulation in CHO M1 stable cell line preincubated with or without potential Gq inhibitors. Depicted are analogs with the highest inhibitory effect (FR, YM, 1, 2), moderate activity (3) and inactive compounds (4, representative for all other inactive derivatives, Table S1 and Figure S6).

### Structural studies by NMR spectroscopy.

Consequently, a concise <sup>1</sup>H-NMR-based characterization of FR, FR analogs 1, 2, and FR-derived peptides 5 and 13 was accomplished in various solvents (water, chloroform, and methanol/water, Tables S3–S9). Additionally, solution structures were calculated from NOE intensities in water for FR and

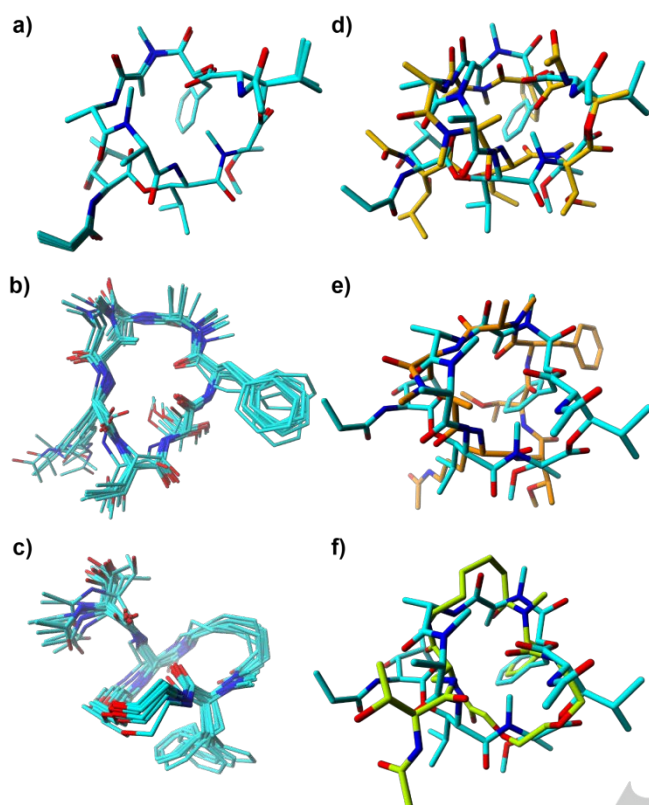


**Figure 2.** Solution NMR structures of a) FR and its analogs b) **5** and c) **13** (presented as ensembles of 10 lowest energy structures (coloring scheme: carbon - cyan, nitrogen - blue, oxygen - red). Superposition of the NMR solution structure of FR (carbon - cyan) with d) YM (PDB ID 3AH8,<sup>[14]</sup> all atom RMSD 2.84 Å, carbon - yellow), e) **5** (all atom RMSD 7.34 Å, carbon - orange), and f) **13** (all atom RMSD 8.48 Å, carbon - green).

peptides **5** and **13** (Figure 2, Tables S3–S5). Similar to YM, chloroform spectra of FR showed two resolved sets of NMR signals, indicating a major and a minor conformation at a ratio of 10:1 at 293 K (Table S3).<sup>[6]</sup> These two conformations are most likely caused by a *cis/trans* isomerization of the amide bond between *N*-MeDha5 and D-Pla6 with the major conformer exhibiting the *trans* amide bond. Apart from the major isomer, a large chemical shift separation of the two H $\beta$  protons of *N*-MeDha5 (5.69; 3.73 ppm vs. 5.32; 5.07 ppm, CDCl<sub>3</sub>, Table S3) was observed which is presumably due to the ring current effect of the nearby phenyl ring of D-Pla6 accounting for a *cis* amide bond. In contrast to the above observations, the minor conformer appears to be the major conformer in aqueous media as revealed by a series of <sup>1</sup>H-NMR spectra at different temperatures in a water/methanol mixture (Figure S7). Moreover, this isomer was the only observable species at 277 K, while multiple minor conformations emerged with increasing temperature as concluded from the appearance of multiple additional signals in the <sup>1</sup>H chemical shift region of 6 to 9 ppm (Figure S7).

Finally, NMR structure calculations clearly confirmed that FR exclusively exists in a well-defined global conformation (ensemble heavy atom RMSD 0.19 Å, Figure 2a, Table S6) in aqueous solution which indeed revealed a *cis* amide bond between D-Pla6 and *N*-MeDha5. All other amide bonds were

identified to be in a *trans* conformation. In contrast, earlier NMR studies on YM254890 in various organic solvents<sup>[13]</sup> indicated *cis* amide bonds between *N*-MeThr8(OMe)/ $\beta$ -HyLeu-2, *N*-MeAla3/Ala4 based on the presence of H $\alpha$ /H $\alpha_{i+1}$  NOE crosspeaks, which were clearly missing in FR. Even though Gq-bound YM (PDB ID 3AH8)<sup>[14]</sup> was found in the same conformation as revealed by NMR in organic solvents,<sup>[13]</sup> the global backbone fold of the cyclic FR-core remained fairly similar. In contrast, the  $\beta$ -HyLeu1/2 tail was found to be in a different orientation and rotated along the  $\beta$ -HyLeu1/2 ester bond by approx. 150° (Figure 2d).

In contrast to FR, analog **5** forms a rather flat cycle (ensemble heavy atom RMSD 0.83 Å, Figure 2b, Table S6) folding into two equally populated conformations showing *cis/trans* isomerism between *N*-MeAla5 and Ala6. A second stable *cis* peptide bond was observed between Ala6 and *N*-MeAla7. In addition, although distinct parts of the structure of **5** (*N*-MeAla5, Ala6, *N*-MeAla7, and Ac-Lys1) are in good agreement with FR (*N*-MeDha5, Ala4, *N*-MeAla3), it deviates to some extent from the solution structure of FR (RMSD 7.35 Å, Figure 2e). Similarly, **13** also folds into a flat cyclic structure (ensemble heavy atom RMSD 0.71 Å, Figure 2c, Table S6), which appears to be more flexible compared to **5** (Figure 2b, c). The structural deviation of **13** from the global conformation of FR, however, is significant (RMSD 8.48 Å, Figure 2f). Thus, **5** and **13** do not reproduce the global fold of FR, which most likely accounts for their lack of biological activity.

#### Molecular modeling and docking studies.

Molecular modeling and docking studies were applied to provide in-depth insight into inhibitor-Gq interactions and to characterize the binding mode of the most potent inhibitors. It is assumed that FR/YM analogs share the same mechanism of inhibition which is achieved by impairing the domain opening motion of the helical and the Ras-domain of the G $\alpha$  subunit preventing the release of the nucleotide GDP.<sup>[14,15]</sup>

The YM-derived analogs **15**, **17–27**, and **29–36**, investigated herein were constructed from the Gq-bound conformation of YM-254890 (PDB ID 3AH8) (Table S10).<sup>[14]</sup> For FR-derived analogs **1–4**, two conformations were built employing the solution NMR structure of FR in water and the Gq-bound conformation of YM.<sup>[14]</sup> The structures obtained were then docked to the heterotrimeric Gq protein in the original conformation (Text S1).<sup>[14]</sup> Except for **23**, which carries a backbone modification (*N*-MeAla3 to Ala), these analogs contain side chain modifications at *N*-MeAla3, Ala4,  $\beta$ -HyLeu1/2 or at the acetyl group of Thr7/ $\beta$ -HyLeu7. A closer look at the target-bound conformation of these analogs obtained from the docking runs revealed only minor alterations of the global fold of the inhibitor molecules retaining the intramolecular hydrogen bonds as observed in YM/FR (Figure S13). Consequently, the best inhibitory analogs **1**, **2**, and **15–23** (Scheme 1b) also share a similar orientation in the FR/YM-binding pocket on Gq resulting in almost identical hydrogen bond interactions with the protein (Figure S13a,b, Tables S10, S11). Moreover, similar orientations as found for YM within the FR/YM-binding pocket on Gq were observed when the alternative NMR-derived structures for FR and **1** (named FR *cis* and **1 cis** thereafter) were employed in the docking experiments (Figure S12a-c). A marginally different Gq-bound orientation concerning the FR/YM-binding pocket was found for the NMR derived structure of **2** (named **2 cis** thereafter,

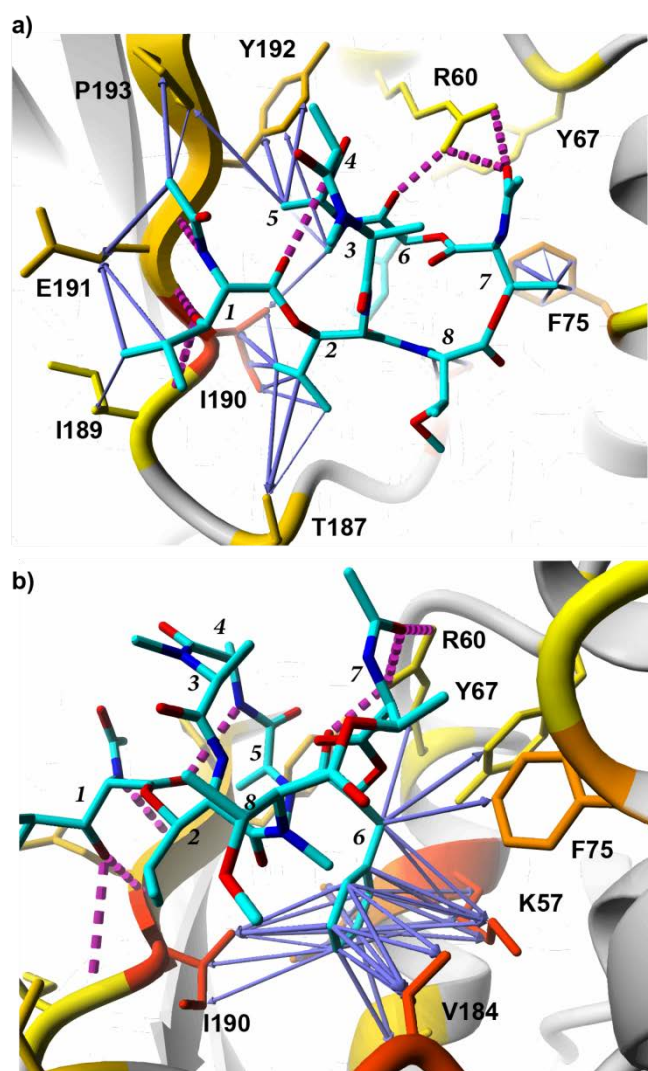


**Figure 3.** a) and b) Illustration of key interactions of best inhibitory compounds (high affinity compounds) exemplarily shown for YM-254890 (residue numbers – italic, coloring scheme: carbon - cyan, nitrogen - blue, oxygen – red) with Gq (residue numbers – regular, bold). b) Network of hydrophobic interactions of *D-Pla* of YM-254890 within the hydrophobic cleft at the interface of the helical and Ras-domain of the G protein. Intra- and intermolecular hydrogen bonds are indicated by magenta dotted lines. Hydrophobic interactions between Gq and inhibitor are depicted by blue arrows between the interacting atom pairs (thickness of arrow indicates interaction strength). Gq residues are colored according to the sum of their hydrophobic interaction energy with the inhibitor, ranging from yellow (1 kJ/mol - weak) to red (10 kJ/mol - strong).

Figure S12d).

In conclusion, this strong orientation towards linker 1 and  $\beta$  sheet 2 of the  $G\alpha$  subunit, mainly represented by the hydrogen bonds to Arg60 and Glu191 and hydrophobic interactions towards segments  $\alpha 1$  (I56, K57),  $\alpha A$  (F75), switch I (V184), and  $\beta$  sheet 2 (I190, Y192, P193), complement intrinsic features of powerful Gq inhibitors based on FR or YM (Figure 3).

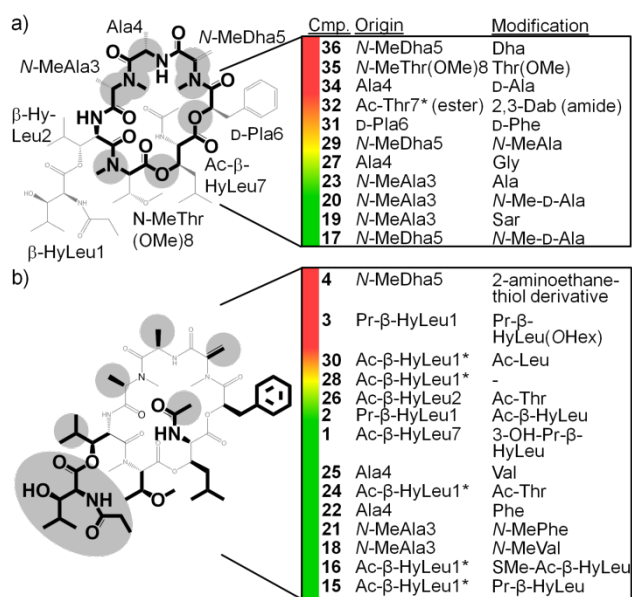
In case of the moderately active analogs **29–31**, each compound appears to be conformationally more flexible compared to YM/FR as revealed by our MD simulations (Figure S8). Thus, these would result in different global conformations compared to the original conformation (Figures S10, S13c) and,

in turn, in different orientations in the FR/YM-binding pocket compared to YM (Figure S13c, Tables S10, S11).

Regarding the less or inactive compounds **3–14** and **32–36** an increased structural flexibility as assessed by NMR analysis and MD simulation (except of **3** and **4**) significantly altered the global conformation resulting in highly dissimilar structures compared to YM/FR (Figure S11). Taking a closer look at the orientation of the less active compounds in the FR/YM-binding pocket on Gq, except of **35**, the phenyl ring of *D-Pla* resides in the hydrophobic cleft as already observed for the best inhibitory and moderately active YM/FR analogs. Another common feature among this group of YM analogs is the tendency of hydrogen bond formation with the switch I region or residues of the  $G\beta$  subunit as shown for **3** and **36** in Figure S13d (Tables S10, S11). However, with the exception of **3** and **32**, Arg60 was no longer linked via hydrogen bonding by any of these analogs. Instead, Arg96 of the  $G\beta$  subunit became a major hydrogen bonding partner. In any case, the modifications introduced into the less active YM/FR analogs significantly altered the conformation of the inhibitor molecule and thus the ability to correctly access the rather deep binding pocket. This interpretation becomes even more valid with respect to the different conformation of the inactive peptides (**5–13**).

#### Deviation of recognition determinants for inhibitor binding to Gq.

FR and YM represent small to medium-sized compounds with a high degree of chemical complexity, specific three-dimensional conformations, and consequently precise orientation of backbone and side chain atoms through intrinsic rigidity. Our attempt focused on characterizing features accounting for the high inhibitory activity of YM/FR towards their specific binding pocket on Gq and on sampling chemical space here to identify possible sites for further optimization. This analysis revealed how changes in three distinct categories affect inhibitory potency compared to the lead compounds, namely I) backbone conformation, II) backbone conformation influencing the intramolecular hydrogen bond network, and III) side chain constitution and orientation (Scheme 2). In analogs belonging to categories I and II, which are based mainly on backbone modifications, most drastic effects or even complete loss of activity were observed in derivatives **36**, **35**, **34**, and **32**, in which only single atoms or small groups were changed at positions 8 (*N*-MeThr(OMe)), 7 (Ac-Thr in YM), 5 (*N*-MeDha), or 4 (Ala) relative to YM/FR (Scheme 1b, 2a). Considering structural alterations within backbone modifications, two different types need to be taken into account: a) sole conformational changes (category I), e.g. evoked by inversion of configuration as in **34**, and b) functional impairment of intramolecular hydrogen bonding (category II), as occurring in **32**, **35**, and **36** (Figure S11). Exploring their individual binding modes revealed perturbations on the individual molecule's integrity with respect to YM/FR and their binding behavior. Substitution of an ester by an amide bond as in **32** was also introduced in a further compound (**31**) at a different position (*D-Pla*6 to *D-Phe*), which turned out to result in a moderately active derivative compared to the inactive **32**, **34–36**. This demonstrates that the ester bond at position 7 is more important concerning the macrocycle's bioactive conformation than the bond at position 6. There was one further modification in the backbone associated with a change in the hydrogen bond network, namely compound **23** (*N*-MeAla3 to Ala), which,



**Scheme 2.** Structural classification of compounds with modifications at one site of FR and/or YM according to their impact on a) backbone and intramolecular hydrogen bonds and b) side-chain modifications, i.e. inactive analogs **5–14** carrying more complex modifications at different sites are not considered here. Coloured bars next to compounds indicate acceptance of modifications (red - inactive compounds with minor, non-tolerated substitutions, yellow - moderately active compounds with partially tolerated substitutions, green - active compounds with tolerated substitutions). \*Nomenclature refers to YM-254890. 2,3-Dab, 2,3-diaminobutyric acid; Sar, sarcosine; SMe-Ac, methylthioacetyl.<sup>[5]</sup>

however, did not significantly change the inhibitory activity compared to YM/FR (Scheme 2a). Finally, concerning backbone modifications only the reduction of *N*-MeDha5 to *N*-MeAla led to a strong effect on activity, which induced stronger changes to the backbone conformation than the *N*-Me-D-Ala substitution. All further alterations as found in **27**, **23**, **20**, **19**, and **17**, including changes such as an increase in flexibility (e.g. Ala4 to Gly, **27**) or the inversion of configuration (*N*-MeAla3 to *N*-Me-D-Ala, **20**), were tolerated (Scheme 2a).

Thus, it is obvious that the surface region of the YM/FR molecule comprising residues *N*-MeAla3 and Ala4 accepts such changes, whereas in the region between *N*-MeDha5 to *N*-MeThr(OMe)8 not even marginal modifications are tolerated, most likely due to their direct interaction with the protein surface. A more detailed analysis of category III comprising primarily side chain modifications and functionalities apart from the backbone atoms revealed a rather different picture: With the exception of the two semisynthetic compounds (**3**, **4**) modified at the *N*-MeDha5 exomethylene group (**4**) or at the Pr-β-HyLeu1 side chain (**3**), other changes were partially or almost completely tolerated compared to the lead structures (Scheme 2b). This can be attributed primarily to the fact that the aforementioned backbone-related criteria are retained in these analogs. In addition, regarding the protein-facing side in YM/FR no alterations were made or identified at residues 6, 7, and 8, whereas at both ends spanning the sequence between residues 5 (*N*-MeDha) and 1, 2 (Ac-β-HyLeu) modifications maybe critical as can be proven with compounds **3**, **4**, **28**, and **30** (Scheme 2). For **3**, **28** and **30**, important hydrogen bond interactions between

the hydroxyl function of Ac-β-HyLeu1 and the Gq backbone at Ile190 and Glu191 are missing, while in case of **4** the bulkiness of semisynthetically prolonged *N*-MeDha5 avoids interactions at the binding site for D-Pla6. If more than one amino acid substitution was introduced at the same time, effects were even more striking. In case of **33**, simultaneous exchange of Ac-β-HyLeu at positions 1 and 2 for Ac-β-Thr led to complete loss of activity at Gq most likely due to their smaller size. With respect to our simulations, this would allow for a reorientation of the two tail residues towards Arg96 at the Gβ subunit not only resulting in the loss of hydrogen bond interaction with Ile190 and Glu191 similar to compounds **3**, **28**, and **30** but also losing hydrophobic contacts in this region. In case of **24** and **26**, in which each of the β-HyLeu residues was mutated to Thr independently, the steric reductions were not sufficient to allow for such reorientations, thus preserving the hydrogen bond interactions with the protein.

## Conclusions

The present report contributes essentially to the understanding of the interaction of potent inhibitors such as depsipeptides FR900359 and YM-254890 within their specific binding pocket on the Gq protein. Together with the analysis of the backbone (categories I and II) it becomes apparent that except of two residues, *N*-MeAla3 and Ala4, the remaining part of the YM/FR molecule represents the “pharmacophore” for this specific binding pocket on Gq (Figure 3). In addition, both molecules obviously represent optimal, highly efficient and specific compounds for Gq inhibition, since none of the natural as well as the artificial modifications yielded more potent analogs so far. It is known that natural products represent structures validated from millions of years of coevolution with their specific target exploiting precision in complementary chemical design.<sup>[22,23]</sup> Hence, it seems unlikely that a significant improvement regarding Gq-inhibitors can be obtained with the limited opportunities provided by the YM/FR template(s), which already serve as suitable chemical tools in basic pharmacological studies.<sup>[24–26]</sup> In terms of perspective, one conceivable task thus could be the implementation of strategies to target other Gα protein subunits based on the YM/FR natural models.

## Experimental Section

**General chemicals and stock solutions.** Reagents for chemical derivatization of FR were purchased from commercial sources and were used without further purification. Oxygen- or water-sensitive reactions were performed under argon atmosphere. Standard coupling reagents (HBTU, HOBt, TFFH, PyBOP), resins and amino acid derivatives used for solid phase synthesis of analogs were purchased from Orpegen Peptide Chemicals GmbH (Heidelberg, Germany), Novabiochem and IRIS Biotech (Marktredwitz, Germany), respectively. Peptide synthesis reagents (piperidine, DIEA, trifluoroacetic acid, BTSa) and solvents (*N,N*-dimethylformamide, dichloromethane) were of reagent grade, and solvents for chromatography (acetonitrile, water, methanol) were of analytical grade obtained from VWR International (Dresden, Germany). Cell culture reagents were purchased from Invitrogen. All other reagents were from Sigma-Aldrich unless stated otherwise.

**Depsipeptide isolation and purification.** Bioassay, LC-MS and <sup>1</sup>H NMR guided fractionation of the crude extracts obtained from the plant

*Ardisia crenata*, yielded the cyclic depsipeptide FR. The investigated plant material was cultivated in the green house of the Botanical Garden Bonn.

200 g of dried plant leaves were coarsely crashed and extracted with methanol. Further purification steps included liquid-liquid extraction, RP-18 vacuum liquid chromatography and size exclusion chromatography. Final purification was done by HPLC with a semi-preparative YMC Hydrosphere RP-18 column (250 x 4.6 mm, 3 μm). The elution system was water (eluent C) and methanol (eluent D). The crude peptide was derived with isocratic conditions (80% eluent D for 35 minutes). The separation of FR from its analogs was achieved using a Nucleoshell RP<sub>18+</sub> column (250 x 8 mm, 5 μm) with isocratic 75% eluent D for 20 minutes, followed by a linear gradient to 100% eluent D in 35 minutes. Pure FR was isolated as a white powder *t<sub>R</sub>*: 28.2 min (10 mg from 200 g dried leaves). The isolation scheme is shown in Figure S2.

**Isolation of natural FR-analogs 1 and 2.** **1** was isolated as described by Crüsemann *et al.*<sup>[3]</sup> HPLC conditions had to be adjusted to separate **2** from **1** (for the complete isolation scheme refer to Figure S2). The composition of the mobile phase was changed from isocratic 80% eluent D to 75 % eluent D applying a 75:25 Nucleoshell RP<sub>18+</sub> column (250 x 8 mm, 5 μm) for 20 minutes followed by a linear gradient from 75–100% eluent D within 15 minutes. The new cyclic depsipeptide, **2**, was obtained as white powder (about 0.2 mg from 200 g dried leaves, *t<sub>R</sub>* = 23.7 min). The isolation process was repeated until 1.6 mg of **2** were collected for structure elucidation.

**Generation of compounds 3 and 4 by chemical derivatization of FR900359.** The synthesized compounds were analyzed by uHPLC-MS/MS on a micrOTOF-Q mass spectrometer (Bruker) with ESI-source coupled with an HPLC Dionex Ultimate 3000 (Thermo Scientific) using a Zorbax Eclipse Plus C18 1.8 μm column, 2.1 x 50 mm (Agilent). The column temperature was 45 °C. MS data were acquired over a range from 100–3000 *m/z* in positive mode. Auto MS/MS fragmentation was achieved with increasing collision energy (35–50 keV over a gradient from 500–2000 *m/z*) with a frequency of 4 Hz for all ions over a threshold of 100. UPLC begins with 90% H<sub>2</sub>O containing 0.1% acetic acid. The gradient started after 0.5 min to 100% acetonitrile (0.1% acetic acid) in 4 min. 2 μL of sample solution was injected to a flow of 0.8 mL/min.

**Compound 3:** (2S,3R)-1-((1R)-1-((6S,9S,12S,18R,21S,22R)-21-acetamido-18-benzyl-22-isopropyl-3-((R)-1-methoxyethyl)-4,9,10,12,16-pentamethyl-15-methylene-2,5,8,11,14,17,20-heptaoxo-1,19-dioxo-4,7,10,13,16-pentaazacyclodocosan-6-yl)-2-methylpropoxy)-4-methyl-1-oxo-2-propionamidopentan-3-yl hexanoate

FR (20 mg, 19.96 μmol) was dissolved in pyridine (1 mL) and stirred at room temperature under argon atmosphere. DMAP (12.2 mg, 99.8 μmol) and hexanoic anhydride (21.4 mg, 99.8 μmol) were added. After 2 h the reaction mixture was heated to 50 °C and stirred. After 16 h at 50 °C the reaction was stopped by diluting with 5 mL water and the reaction mixture was extracted with CH<sub>2</sub>Cl<sub>2</sub> (3 mL x 3). The combined organic layers were washed with solutions of NaHCO<sub>3</sub> (pH 9), KHSO<sub>4</sub> (pH 2) and saturated NaCl and afterwards dried over Na<sub>2</sub>SO<sub>4</sub> and concentrated in vacuo. Crude peptide was purified by HPLC, YMC Hydrosphere C18 column (250 x 4.6 mm, 3 μm). The elution system was 0.05% TFA in water (eluent E) and 0.05% TFA in acetonitrile (eluent F). A linear gradient was applied from 70% eluent F to 100% eluent F in 30 minutes. **3** eluted at *t<sub>R</sub>* = 13.1 min and after solvent evaporation appeared as white-yellow powder (2.6 mg).

**Compound 4:** (2S,3R)-1-((1R)-1-((6S,9S,12S,18R,21S,22R)-21-acetamido-15-(((2-aminoethyl)thio)methyl)-18-benzyl-22-isopropyl-3-((R)-1-methoxyethyl)-4,9,10,12,16-pentamethyl-2,5,8,11,14,17,20-heptaoxo-1,19-dioxo-4,7,10,13,16-pentaazacyclodocosan-6-yl)-2-methylpropyl 3-hydroxy-4-methyl-2-propionamidopentanoate

To a micellar solution of SDS (1 mL), at the critical micelle concentration (CMC) = 8.1 x 10<sup>-3</sup> M, FR (20 mg, 19.96 μmol) and 2-aminoethanethiol hydrochloride (26.7 mg, 199.6 μmol) were added at room temperature. The mixture was stirred vigorously (800 rpm) and monitored by TLC until the starting material had been consumed after 12 h. Then the mixture was extracted with *n*-butanol (3 mL x 3). The combined organic layer was dried over Na<sub>2</sub>SO<sub>4</sub> and concentrated in vacuo. The crude peptide mixture was purified by HPLC, Nucleoshell RP<sub>18+</sub> column (250 x 4.6 mm, 5 μm). The elution system was water (eluent C) and methanol (eluent D). **4** elutes at *t<sub>R</sub>* = 27.2 minutes using isocratic conditions (57% eluent D for 35 minutes) and appears as transparent film (6 mg) after solvent evaporation.

**Synthesis of Fmoc-β-HyLeu-OH.** For the preparation of Fmoc-β-HyLeu-OH, a mixture of H-β-HyLeu-OH (1 equiv.) in DCM was stirred while bis(trimethylsilyl)acetamide (6 equiv.) was added dropwise over a duration of 15 min at room temperature until complete dissolution and allowed to stir for further 2 h. The solution was cooled to 0 °C and DIEA (1.25 equiv.) added at once. Under vigorous stirring Fmoc-Cl (1.25 equiv.) was added in portions for a duration of 30 min while stirring at 0 °C. This was continued for 1 h on ice and further 4 h at room temperature. The solvent was removed and the crude product (oil) was dissolved in ethyl acetate and washed with salt solutions of 5% KHSO<sub>4</sub>, saturated NaCl (brine), saturated NaHCO<sub>3</sub>, and again with brine. The ethyl acetate was dried with sodium sulphate (anhydrous) and then filtered. The solvent was removed and the product redissolved in 80% *t*-BuOH. Subsequent freeze-drying gave Fmoc-β-HyLeu-OH (48%) as a white powder. Purity was confirmed by analytical HPLC using a Vydac 218TP54 column (C18, 5 μm particle size, 300 Å pore size, 4.6 mm x 25 mm) and a gradient of 20% to 80% acetonitrile in water with 0.1% TFA in one hour (*t<sub>R</sub>* = 29.86 min). Further Characterization of the product was performed by mass spectrometry, NMR spectroscopy and thin layer chromatography (TLC).

MS (ESI): mass calculated for C<sub>21</sub>H<sub>23</sub>NO<sub>5</sub>, 369.2; *m/z* found, 370.2 [M+H]<sup>+</sup>. <sup>1</sup>H NMR (600 MHz, CDCl<sub>3</sub>) δ ppm 0.92 (d, *J* = 6.6 Hz, 3H), 1.02 (d, *J* = 6.6 Hz, 3H), 1.80–1.71 (m, 1H), 3.82 (dd, *J* = 9.2, 1.1 Hz, 1H), 4.19 (t, *J* = 7.2 Hz, 1H), 4.36 (dd, *J* = 7.2, 4.7 Hz, 2H), 4.58 (dd, *J* = 9.4, 1.2 Hz, 1H), 4.84 (br s, 1H), 5.94 (d, *J* = 9.4 Hz, 1H), 7.27 (dd, *J* = 7.4, 7.4 Hz, 2H), 7.40–7.33 (m, 2H), 7.57 (dd, *J* = 11.7, 7.5 Hz, 2H), 7.73 (dd, *J* = 7.5, 2.3 Hz, 2H). <sup>13</sup>C NMR (151 MHz, CDCl<sub>3</sub>, T = 298 K) δ ppm 19.0, 19.3, 30.9, 47.2, 56.3, 67.5, 77.5, 120.1 (2C), 125.3, 125.3, 127.2 (2C), 127.8 (2C), 141.4 (2C), 143.7, 144.0, 157.2, 175.7. TLC was performed using glass plates impregnated with silica gel 60 F254, 10 x 20 cm. The applied solvent system was chloroform/methanol (9:1). Detection was done by UV at a wavelength of 254 nm. The observed R<sub>f</sub> value was 0.83.

**Peptide synthesis and purification.** The linear precursor peptides of **7**, **8**, **11**, and **12** were synthesized on an automated peptide synthesizer EPS 221 (Intavis Bioanalytical Instruments AG, Cologne, Germany) according to a standard Fmoc-protocol. Peptides **5**, **6**, **9**, **10**, **13**, and **14** were synthesized manually. The polymer support was 2-chlorotrityl chloride resin with a loading capacity of 2.1 mmol/g (Advanced ChemTech 5609 Fern Valley Road, Louisville KY, USA) for manual peptide synthesis or alanine-loaded 2-chlorotrityl chloride resin with a loading capacity of 0.67 mmol/g (Iris Biotech GmbH, Marktredwitz, Germany) for automated peptide synthesis. Amino acid derivatives used were as follows: Fmoc-*N*-Me-Thr(*t*Bu)-OH; Ac-Thr-OH; Fmoc-*N*-Me-Ala-OH; Fmoc-Lys(Ac)-OH and Fmoc-Thr(Ac)-OH, Fmoc-*N*-Me-D-Phe-OH, Fmoc-6-Ahx-OH, Boc-Dap(Fmoc)-OH and Fmoc-Leu-OH, Fmoc-β-HyLeu-OH.

For manual peptide synthesis, coupling reactions were performed as double couplings using Fmoc-amino acids (4 equiv.) activated with TFFH (4 equiv.) for 12 min, in the presence of DMF and DIPEA (8 equiv.). Fmoc removal was carried out by treating the resin twice with 20% of piperidine in DMF for 5 and 15 min, respectively. All deprotection and coupling steps were followed by intensive washings using DMF and DCM

alternately. Peptide cleavage and deprotection was accomplished with 5% TIPS in 95% TFA/H<sub>2</sub>O for peptides **5–14** for 3 h at room temperature. The crude peptides were precipitated in cold diethyl ether, centrifuged and washed with diethyl ether several times. Linear peptides were of sufficient purity and subsequently used without prior purification for the following steps. The peptide cyclization was performed using PyBOP (6 equiv.) and DIEA (12 equiv.) in DMF (final concentration of peptides: 320 μM) for 6 h at room temperature.

The crude peptides were evaporated and then purified by semi-preparative reversed-phase HPLC using a Shimadzu LC-8A system (Duisburg, Germany) equipped with a C18 column (250 × 32 mm, Knauer Eurospher 100, Berlin, Germany). The gradient elution system was 0.1% TFA in water (eluent A) and 0.1% TFA in acetonitrile/water (9:1) (eluent B). The peptides were eluted with varying gradients of eluent B in eluent A in 120 min as depicted in Table S2 and a flow rate of 10 mL/min. The peaks were detected at 220 nm. Collected fractions were combined, freeze-dried and stored at -20 °C. Purity of the peptides was confirmed by analytical reversed-phase HPLC on a Shimadzu LC-10AT chromatograph (Duisburg, Germany) equipped with a Vydac 218TP54 column (C18, 5 μm particle size, 300 Å pore size, 4.6 mm × 25 mm). The peptides were eluted with varying gradients as noted in Table S2. The flow rate was 1 mL/min with eluent A: 0.1% TFA in water and eluent B: 0.1% TFA in acetonitrile; detection was at 220 nm. All peptides used for biological assays were of >95% HPLC purity.

**Chemical characterization of FR-analogs.** Peptides were characterized by analytical HPLC (see above), amino acid analysis, and mass spectrometry (Table S2). For amino acid analysis, samples (0.5–1 mg) were hydrolyzed in 6 N HCl at 110 °C for 24 h, dried and used for analysis in sample dilution buffer (Onken Laboratories, Hamburg, Germany) on an Eppendorf Biotronik Amino Acid Analyzer LC3000. The molecular weight of crude and purified peptides **5–14** was confirmed by mass spectrometry on an ESI micrOTOFQ III system (Bruker Daltonics GmbH, Bremen, Germany).

TLC characterization was performed using glass plates impregnated with silica gel 60 F254, 10 × 20 cm. Two solvent systems were applied, which were; system A: *n*-butanol/acetic acid/water (48:18:24) and system B: *n*-propanol/ 25% NH<sub>3</sub> (7:3). Detection methods used were UV at a wavelength of 254 nm and KI-containing acetic *o*-tolidin solution.

The molecular formula of **2** was determined to be C<sub>48</sub>H<sub>73</sub>N<sub>7</sub>O<sub>15</sub>, based on HR-FTICR mass measurements (calcd. 988.5237; obsd. 988.5236) for [M+H]<sup>+</sup>. Compared with FR, compound **2** thus had a molecular mass 14 Da lower, suggesting **2** to have a methylene group less in its structure. Sequential fragmentation of the depsipeptide **2** via collision induced dissociation demonstrated the close structural similarities between FR and **2**, and further indicated that **2** differs from FR regarding the acyl residue of *N*-propionylhydroxy-leucine of FR (Figure S3). In general, compounds FR, **1**, and **2** have similar MS fragmentation patterns. The compounds can be distinguished by characteristic  $\Delta m/z$  values resulting from modified amino acids. In the first fragmentation step compound **2** loses the side chain, which can be seen in the MS spectra as a 171.10 Da fragment (*N*-Ac- $\beta$ -HyLeu). Instead, for FR a  $m/z$  185.11 Da fragment, i.e. *N*-propionyl- $\beta$ -hydroxy-leucine is cleaved off. Comparison of further fragments also proved that in compound **2** the *N*-acyl residue at C-42 is different (see also Figure S3). These MS data together with extensive NMR spectral data analysis (<sup>1</sup>H, <sup>13</sup>C, <sup>1</sup>H-<sup>1</sup>H-COSY, <sup>1</sup>H-<sup>13</sup>C-HSQC, <sup>1</sup>H-<sup>13</sup>C-HMBC) let us conclude for **2** that an acetic acid moiety is placed at the side chain  $\beta$ -HyLeu residue instead of propionic acid (as in FR).

Evidence was provided from (i) the lacking NMR signals for a propionate methylene CH<sub>2</sub>-48, at  $\delta_{\text{H}}$  2.57 and  $\delta_{\text{H}}$  2.50 /  $\delta_{\text{C}}$  28.2 and a methyl moiety CH<sub>3</sub>-49 at  $\delta_{\text{H}}$  1.19 /  $\delta_{\text{C}}$  10.1, respectively (as compared to FR, Table S3), (ii) the additional NMR signals for the acetate methyl group CH<sub>3</sub>-48 at  $\delta_{\text{H}}$  2.24 /  $\delta_{\text{C}}$  22.7, (1D-NMR and HSQC spectral data of **2**), as well as (iii) the HMBC correlation of methyl group resonance CH<sub>3</sub>-48 to that of the

neighboring amide carbonyl group (C-47,  $\delta_{\text{C}}$  171.4, Table S9). The position of the acetate moiety at NH-42 was evident from HMBC correlations between the resonance for NH-42 ( $\delta_{\text{H}}$  7.27) and that of C-47 ( $\delta_{\text{C}}$  171.4). Further evidence for the site of modification of **2** as compared to FR came from LCMS<sup>2</sup> experiments (Figure S3).

The molecular formula of **3** was determined to be C<sub>55</sub>H<sub>85</sub>N<sub>7</sub>O<sub>16</sub> (calcd. 1122.5945; obsd. 1122.5952) for [M+Na]<sup>+</sup>. This result from an accurate mass measurement, which showed a mass difference of 98Da between FR900359 and compound **3**, suggesting the successful esterification of the secondary alcohol of the *N*-propionylhydroxy-leucine (L<sup>'''</sup>) residue of FR with hexanoic anhydride to the corresponding L<sup>^</sup> = *N*-propionyl-(2S,3R)-3-(hexanoxyloxy)-hydroxy-leucine moiety of **3**. Mass spectrometric analysis, especially when comparing fragments from sequential fragmentation via collision induced dissociation of the depsipeptides FR and **3** demonstrated that **3** differs from FR regarding the L<sup>'''</sup> moiety of FR, as expected (Figure S4). The compounds can be distinguished by different  $\Delta m/z$  values of the modified amino acids. For **3** this is evident from the second-generation mass spectra of  $m/z$  993.51 compared with the 98 Da lower weight  $m/z$  895.45 for FR. Loss of the sidechain L<sup>'''</sup> (FR,  $\Delta m/z$  185.11 Da) or L<sup>^</sup> (**3**,  $\Delta m/z$  283.17 Da), respectively leads for both compounds to the same fragment  $m/z$  710.34 Da (Figure S4).

The molecular formula of **4** was determined to be C<sub>51</sub>H<sub>82</sub>N<sub>6</sub>O<sub>15</sub>S (calcd. 1079.5693; obsd. 1079.5710) for [M+H]<sup>+</sup>. This result from an accurate mass measurement, which showed a mass difference of 77.03 Da between the molecular ions of FR and compound **4**, suggested the successful addition of 2-aminoethanethiol to the *N*-methyldehydroalanine (A<sup>''</sup>) moiety of FR. Mass spectrometric analysis, especially when comparing fragments from sequential fragmentation via collision induced dissociation of the depsipeptides FR and **4** indeed demonstrated that **4** differs from FR regarding the *N*-methyldehydroalanine (A<sup>''</sup>) moiety, as expected (Figures S3, S5a). Instead of the latter, compound **4** contains an *N*-methyl-3-((2-aminoethyl)thio)-2-alanine moiety, which was revealed from comparison of the LCMS<sup>2</sup> data (Figure S3) of FR and **4**. For compound **4** a loss of  $\Delta m/z$  77.03 Da referring to a 2-aminoethanethiol moiety is observed, e.g. fragmentation of the ion at  $m/z$  309.13 results in a loss of 77.03 Da to yield  $m/z$  232.10. The latter represents the A<sup>''</sup>-F<sup>'</sup>-dipeptide occurring in both peptides, **4** and FR. Comparison of further fragments strengthen this posit (Figure S3). The conjugation of 2-aminoethanethiol to FR seems to give stereospecifically one epimer of the conjugate because of a single peak in the extracted ion chromatogram (Figure S5b), but the configuration at C-5 of compound **4** was not determined. The stereospecificity of Michael reactions were also described by similar conjugation reactions of *N*-methyldehydroalanine moieties of microcystins.<sup>[27–29]</sup> Miles *et al.* explained the stereoselectivity of the reaction with the steric effect of the *N*-methyl group of *N*-methyldehydroalanine, which prohibits the attack of C-5 from two sides.

**NMR spectroscopy.** NMR spectra of FR, **1**, **5**, and **13** were recorded in 90% H<sub>2</sub>O/10% D<sub>2</sub>O, using the freeze-dried solid compound at 298 K on a Bruker Avance III or Avance HD spectrometers at proton frequencies of 600 or 500 MHz. In all NMR spectra, the <sup>1</sup>H peak from water was used as a chemical shift reference by setting its frequency at 4.7 ppm. All NMR data were processed and analyzed using TopSpin 3.1 (Bruker) and CcpNMR Analysis.<sup>[30]</sup> The proton resonance assignment was performed by a combination of 2D [<sup>1</sup>H,<sup>1</sup>H]-DQF-COSY, [<sup>1</sup>H,<sup>1</sup>H]-TOCSY, [<sup>1</sup>H,<sup>1</sup>H]-NOESY and/or [<sup>1</sup>H,<sup>1</sup>H]-ROESY and [<sup>1</sup>H,<sup>13</sup>C]-HSQC. Distance constraints were extracted from [<sup>1</sup>H,<sup>1</sup>H]-NOESY (**13** and FR) or [<sup>1</sup>H,<sup>1</sup>H]-EASY ROESY (**5**) spectra acquired with a mixing time of 120 ms and a recycle delay time of 1.5 s. Upper limit distance constraints were calibrated according to their intensity in the NOESY spectrum and the intensity of geminal protons was used for peak intensity calibration. Torsion angle constraints for FR, **5** and **13** were obtained from <sup>1</sup>H and <sup>13</sup>C chemical shift analysis using DANGLE and <sup>3</sup>J<sub>NH-Ha</sub>-coupling constants.<sup>[31]</sup> Structure calculations and refinements were performed with YASARA structure.<sup>[32–34]</sup> The 10 structures with the lowest energy were selected to represent the NMR solution structures (Figure 2a–c, Table S6). Additionally, a set

of NMR spectra of FR and **1** in CDCl<sub>3</sub><sup>[3]</sup> and MeOH/H<sub>2</sub>O/D<sub>2</sub>O (v:v:v/1:1:0.2) was obtained.

### Molecular modeling and docking studies

**Structures of YM-254890, FR900359 and their analogs.** Molecular structures of the YM and FR derivatives were constructed with the YASARA molecular modeling program<sup>[32,33]</sup> employing the crystal structure of Gq-bound YM.<sup>[14]</sup> The resulting molecules were geometry optimized with the YASARA YAPAC module using semi-empirical quantum chemical methods followed by an energy minimization step in explicit water, using the PME method<sup>[35]</sup> and a cut-off distance of 8 Å to describe long-range electrostatics and the YASARA2<sup>[36]</sup> force field (0.9% NaCl, 298 K, pH 7.4<sup>[37]</sup>). Additionally, selected structures were equilibrated through a 100 ns molecular dynamics simulation to probe for their conformational integrity (Figures S10, S11). The final structure was derived from the simulation period suggesting a stable conformation as indicated by the Cα RMSD, again followed by an energy minimization.

**Molecular Docking Studies.** The Gαq target structure was derived from PDB ID 3AH8.<sup>[14]</sup> Docking was performed using Vina<sup>[38]</sup> (default parameters). The setup was done with the YASARA molecular modeling program,<sup>[32,33]</sup> and the best scoring result of 32 independent docking runs was subjected to further analysis. To guide the docking runs the docking cell was placed around the YM/(FR) binding epitope revealed by Nishimura *et al.*<sup>[14]</sup> Ligands and receptor residues were kept flexible during the docking runs.

**Molecular dynamics simulations.** Energy minimization was carried out for best scoring structures from the docking runs before subsequent analysis of Gαq-inhibitor interactions. The energy minimization was achieved by a steepest-descent minimization followed by a simulated annealing minimization until convergence (<0.05 kJ/mol/200/steps). Charged amino acids were assigned according to the predicted pK<sub>a</sub> of the amino acid side chains by Ewald summation<sup>[37]</sup> and were neutralized by adding counter ions (NaCl). Force field parameters for the ligands were assigned by YASARA's AutoSMILES approach.<sup>[39,40]</sup>

To gain performance, a multiple time step algorithm together with a simulation time step interval of 2.5 fs was chosen.<sup>[32,41]</sup> Unless otherwise stated TIP3P water model and the Amber14 force field was used for energy minimization and molecular dynamics simulations<sup>[42,43]</sup> employing the PME method<sup>[35]</sup> to describe long-range electrostatics at a cut-off distance of 8 Å at physiological conditions (0.9% NaCl, 298 K, pH 7.4<sup>[37]</sup>).

Molecular graphics were created with YASARA ([www.yasara.org](http://www.yasara.org)) and POVRay ([www.povray.org](http://www.povray.org)).

**Cell lines and culture conditions.** CHO and HEK293 cells were obtained from the American Type Culture Collection (ATCC). CHO cells were cultivated in Ham's F12 Nutrient Mix (Ham's F12) supplemented with GlutaMax, 10% fetal bovine serum (PAN biotech, Germany), 100 U mL<sup>-1</sup> Penicillin, 100 mg mL<sup>-1</sup> Streptomycin (Invitrogen). For CHO-M1 cells, 0.2 mg mL<sup>-1</sup> G418 was added to the medium. Cells were maintained in humidified atmosphere at 37 °C and 5% CO<sub>2</sub>. HEK293 cells were cultured in Dulbecco's Modified Eagle's Medium (DMEM, Invitrogen). All cell lines were tested negative by PCR for mycoplasma contamination.

**HTRF-based IP<sub>1</sub> and cAMP assays.** All homogenous time-resolved fluorescence (HTRF)-based assays were carried out according to manufacturer's instructions (Cisbio GmbH, Berlin). In brief, for the IP<sub>1</sub>/cAMP assay, 50,000 cells/well were suspended in the respective assay buffers containing 10 mM LiCl (for IP<sub>1</sub>) or 1 mM 3-isobutyl-1-methylxanthine (IBMX, for cAMP), respectively, and incubated in a 384-well, white microtiter plate for 15 minutes. To determine inhibitory effects of compounds cells were pre-incubated with ligands or solvent for 2 hours prior to stimulation with the stated agonists for further 30–35

minutes (100 μM Carbachol for IP<sub>1</sub>, Gq; 1 μM Iperoxo for cAMP, Gi; 100 μM Iper-6-phth for cAMP, Gs). Reactions were terminated by addition of lysis buffer containing the HTRF® reagents. All incubation steps were carried out at 37 °C and 5% CO<sub>2</sub>. After incubation for at least 1 hour at room temperature HTRF ratios were measured using the Mithras LB 940 multimode reader (Berthold technologies) at 665 nm and 620 nm.

**CellTiter-Blue cell viability assay.** Viability of CHO cells after addition of the respective compounds was assessed using a fluorimetric detection of resorufin formation (CellTiter-Blue, Promega, Mannheim) according to the manufacturer's instructions. Briefly, cells were suspended in cell culture medium (50,000 cells/80 μL/well) and incubated in poly-D-lysine (PDL) treated, 96-well, black, clear-bottom microtiter plates for 4 hours to allow the cells to adhere to the plate. Cells were treated with 20 μL of compound or the respective solvent and incubated for 24 hours at 37 °C and 5% CO<sub>2</sub>. The next day, 20 μL of CellTiter-Blue reagent was added to each well and cells were incubated for 1–3 hours before fluorescence was measured using the Flexstation 3 multimode plate reader (Molecular Devices) at an excitation of 560 nm and emission of 590 nm.

### Acknowledgements

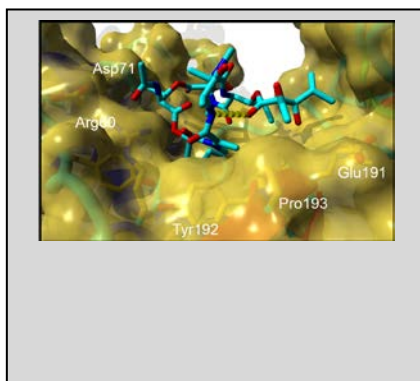
Financial support by the Deutsche Forschungsgemeinschaft within FOR2372 (to D.I., E.K., G.K., and D.T.) is gratefully acknowledged.

**Keywords:** Gα proteins • Gα protein inhibitor • depsipeptides • macrocyclic peptides • NMR structure

### References:

- [1] A. J. Kimple, D. E. Bosch, P. M. Giguère, D. P. Siderovski, *Pharm. Rev.* **2011**, *63*, 728-749.
- [2] D. G. Lambright, J. Sondek, A. Bohm, N. P. Skiba, H. E. Hamm, P. B. Sigler, *Nature* **1996**, *379*, 311-319.
- [3] M. Crüsemann, R. Reher, I. Schamari, A. O. Brachmann, T. Ohbayashi, M. Kuschak, D. Malfacini, A. Seidinger, M. Pinto-Carbó, R. Richarz, T. Reuter, S. Kehraus, A. Hallab, M. Attwood, H. B. Schiöth, P. Mergaert, Y. Kikuchi, T. F. Schäberle, E. Kostenis, D. Wenzel, C. E. Müller, J. Piel, A. Carlier, L. Eberl, G. M. König, *Angew. Chem. Int. Ed.* **2018**, *57*, 836-840.
- [4] H. Zhang, X. F. Xiong, M. W. Boesgaard, C. R. Underwood, H. Bräuner-Osborne, K. Strømgaard, *ChemMedChem* **2017**, *12*, 830-834.
- [5] M. Taniguchi, K. Suzumura, K. Nagai, T. Kawasaki, J. Takasaki, M. Sekiguchi, Y. Moritani, T. Saito, K. Hayashi, S. Fujita, S. Tsukamoto, K. Suzuki, *Bioorg. Med. Chem.* **2004**, *12*, 3125-3133.
- [6] X. F. Xiong, H. Zhang, C. R. Underwood, K. Harpsøe, T. J. Gardella, M. F. Wöldike, M. Mannstadt, D. E. Gloriam, H. Bräuner-Osborne, K. Strømgaard, *Nat. Chem.* **2016**, *8*, 1035-1041.
- [7] H. Kaur, P. W. Harris, P. J. Little, M. A. Brimble, *Org. Lett.* **2015**, *17*, 492-495.
- [8] D. T. Rensing, S. Uppal, K. J. Blumer, K. D. Moeller, *Org. Lett.* **2015**, *17*, 2270-2273.
- [9] A. V. Smrcka, *Trends Pharmacol. Sci.* **2013**, *34*, 290-298.
- [10] M. Fujioka, S. Koda, Y. Morimoto, K. Biemann, *J. Org. Chem.* **1988**, *53*, 2820-2825.
- [11] A. Schmitz, R. Schrage, E. Gaffal, T. H. Charpentier, J. Wiest, G. Hiltensperger, J. Morschel, S. Hennen, D. Häußler, V. Horn, D. Wenzel, M. Grundmann, K. M. Büllsbach, R. Schröder, H. H. Brewitz, J. Schmidt, J. Gomeza, C. Galés, B. K. Fleischmann, T. Tüting, D. Imhof, D. Tietze, M. Gütschow, U. Holzgrave, J. Sondek, K. Harden, K. Mohr, E. Kostenis, *Chem. Biol.* **2014**, *21*, 890-902.
- [12] M. Taniguchi, K. Nagai, N. Arai, T. Kawasaki, T. Saito, Y. Moritani, J. Takasaki, K. Hayashi, S. Fujita, K. Suzuki, S. Tsukamoto, *J. Antibiot. (Tokyo)* **2003**, *56*, 358-363.

- [13] M. Taniguchi, K. Suzumura, K. Nagai, T. Kawasaki, T. Saito, J. Takasaki, K. Suzuki, S. Fujita, S. Tsukamoto, *Tetrahedron* **2003**, *59*, 4533-4538.
- [14] A. Nishimura, K. Kitano, J. Takasaki, M. Taniguchi, N. Mizuno, K. Tago, T. Hakoshima, H. Itoh, *Proc. Natl. Acad. Sci. USA* **2010**, *107*, 13666-13671.
- [15] R. Schrage, A. L. Schmitz, E. Gaffal, S. Annala, S. Kehraus, D. Wenzel, K. M. Bülesbach, T. Bald, A. Inoue, Y. Shinjo, S. Galandrin, N. Shridhar, M. Hesse, M. Grundmann, N. Merten, T. H. Charpentier, M. Martz, A. J. Butcher, T. Slodczyk, S. Armando, M. Effern, Y. Namkung, L. Jenkins, V. Horn, A. Stößel, H. Dargatz, D. Tietze, D. Imhof, C. Galés, C. Drewke, C. E. Müller, M. Hölzel, G. Milligan, A. B. Tobin, J. Gomez, H. G. Dohlman, J. Sondek, K. Harden, M. Bouvier, S. A. Laporte, J. Aoki, B. K. Fleischmann, K. Mohr, G. M. König, T. Tüting, E. Kostenis, *Nat. Commun.* **2015**, *6*, 10156.
- [16] A. Carlier, L. Fehr, M. Pinto-Carbó, T. F. Schäberle, R. Reher, S. Dessen, G. M. König, L. Eberl, *Environ. Microbiol.* **2016**, *18*, 2507-2522.
- [17] T. Kawasaki, M. Taniguchi, Y. Moritani, K. Hayashi, T. Saito, J. Takasaki, K. Nagai, O. Inagaki, H. Shikama, *Thromb. Haemost.* **2003**, *90*, 406-413.
- [18] L. Vallar, A. Spada, G. Giannattasio, *Nature* **1987**, *330*, 566-568.
- [19] H. Bazin, M. Préaudat, E. Trinquet, G. Mathis, *Spectrochim. Acta A Mol. Biomol. Spectrosc.* **2001**, *57*, 2197-2211.
- [20] R. D. Süssmuth, A. Mainz, *Angew. Chem. Int. Ed.* **2017**, *56*, 3770-3821.
- [21] D. Besser, B. Müller, P. Kleinwächter, G. Greiner, L. Seyfarth, T. Steinmetzer, O. Arad, S. Reissmann, *J. Prakt. Chem.* **2000**, *342*, 537-545.
- [22] F. E. Koehn, G. T. Carter, *Nat. Rev. Drug Discov.* **2005**, *4*, 206-220.
- [23] A. L. Harvey, R. Edrada-Ebel, R. J. Quinn, *Nat. Rev. Drug Discov.* **2015**, *14*, 111-129.
- [24] K. Klepac, A. Kilic, T. Gnad, L. M. Brown, B. Herrmann, A. Wildermann, A. Balkow, A. Glöde, K. Simon, M. E. Lidell, M. J. Betz, S. Enerbäck, J. Wess, M. Freichel, M. Blüher, G. M. König, E. Kostenis, P. A. Insel, A. Pfeifer, *Nat. Commun.* **2016**, *7*, 10895.
- [25] M. Matthey, R. Roberts, A. Seidinger, A. Simon, R. Schröder, M. Kuschak, S. Annala, G. M. König, C. E. Müller, I. P. Hall, E. Kostenis, B. K. Fleischmann, D. Wenzel, *Sci. Transl. Med.* **2017**, *2*, 407.
- [26] M. Grundmann, N. Merten, D. Malfacini, A. Inoue, P. Preis, K. Simon, N. Rüttiger, N. Ziegler, T. Benkel, N. K. Schmitt, S. Ishida, I. Müller, R. Reher, K. Kawakami, A. Inoue, U. Rick, T. Kühl, D. Imhof, J. Aoki, G. M. König, C. Hoffmann, J. Gomez, J. Wess, E. Kostenis, *Nat. Commun.* **2018**, *9*, 341.
- [27] C. O. Miles, M. Sandvik, H. E. Nonga, T. Rundberger, A. L. Wilkins, F. Rise, A. Ballot, *Environ. Sci. Technol.* **2012**, *46*, 8937-8944.
- [28] F. Kondo, Y. Ikay, H. Oka, M. Okumura, N. Ishikawa, K. Harada, K. Matsuura, H. Murata, M. Suzuki, *Chem. Res. Toxicol.* **1992**, *5*, 591-596.
- [29] I. Zemskov, H. M. Kropp, V. Wittmann, *Chemistry* **2016**, *22*, 10990-10997.
- [30] W. F. Vranken, W. Boucher, T. J. Stevens, R. H. Fogh, A. Pajon, M. Llinas, E. L. Ulrich, J. L. Markley, J. Ionides, E. D. Laue, *Proteins* **2005**, *59*, 687-696.
- [31] M.-S. Cheung, M. L. Maguire, T. J. Stevens, R. W. Broadhurst, *J. Magn. Reson.* **2010**, *202*, 223-233.
- [32] E. Krieger, G. Vriend, *J. Comput. Chem.* **2015**, *36*, 996-1007.
- [33] E. Krieger, G. Vriend, *Bioinformatics* **2014**, *30*, 2981-2982.
- [34] E. Harjes, S. Harjes, S. Wohlgemuth, K. H. Müller, E. Krieger, C. Herrmann, P. Bayer, *Structure* **2006**, *14*, 881-888.
- [35] U. Essmann, L. Perera, M. L. Berkowitz, T. Darden, H. Lee, L. G. Pedersen, *J. Chem. Phys.* **1995**, *103*, 8577-8593.
- [36] E. Krieger, K. Joo, J. Lee, J. Lee, S. Raman, J. Thompson, M. Tyka, D. Baker, K. Karplus, *Proteins: Struct. Funct. Bioinform.* **2009**, *77*, 114-122.
- [37] E. Krieger, J. E., Nielsen, C. A. Spronk, G. Vriend, *J. Mol. Graph. Model.* **2006**, *25*, 481-486.
- [38] O. Trott, A. J. Olson, *J. Comput. Chem.* **2010**, *31*, 455-461.
- [39] J. Wang, R. M. Wolf, J. W. Caldwell, P. A. Kollman, D. A. Case, *J. Comput. Chem.* **2004**, *25*, 1157-1174.
- [40] A. Jakalian, D. B. Jack, C. I. Bayly, *J. Comput. Chem.* **2002**, *23*, 1623-1641.
- [41] H. Grubmüller, P. Tavan, *J. Comput. Chem.* **1998**, *19*, 1534-1552.
- [42] J. A. Maier, C. Martinez, K. Kasavajhala, L. Wickstrom, K. E. Hauser, C. Simmerling, *J. Chem. Theory Comput.* **2015**, *11*, 3696-3713.
- [43] V. Hornak, R. Abel, A. Okur, B. Strockbine, A. Roitberg, C. Simmerling, *Proteins* **2006**, *65*, 712-725.

**Entry for the Table of Contents**

FR9003590 and YM-254890 are currently the most potent Gq inhibitors known. We report why it is so difficult to improve their potency based on novel FR900359-derivatives and in comparison to all existing analogs. In a combined structural and computational study we identify the binding determinants for these inhibitors in their specific binding pocket on the Gq protein.